Semiconductor Physics, Quantum Electronics & Optoelectronics, 2017. V. 20, N 1. P. 74-78.
doi: https://doi.org/10.15407/spqeo20.01.074

PACS 71.20.Nr, 71.35.Cc, 72.15.Rn, 72.20.Ee, 72.20.Jv, 72.30.+q, 72.40.+w, 73.20.At

Influence of the composition of $(TlGaS_2)_{1-x}(TlInSe_2)_x$ solid solutions on their physical properties

S.N. Mustafaeva, S.G. Jafarova, E.M. Kerimova, N.Z. Gasanov, S.M. Asadov
Institute of Physics, National Academy of Sciences of Azerbaijan
AZ–1143, G. Javid Pr., 131, Baku, Azerbaijan
Tel.: (99412) 539-59-13; Fax: (99412) 539-59-61
E-mail: solmust@gmail.com

Abstract. The single crystals of $(TlGaS_2)_{1-x}(TlInSe_2)_x$ (x = 0…0.5) solid solutions have been grown up. The photoelectric, X-ray dosimetric, dielectric and optical characteristics of the $(TlGaS_2)_{1-x}(TlInSe_2)_x$ solid solutions with various compositions have been determined. The maximum and spectral range of photosensitivity were found to redshift as x increases from 0 to 0.5. Both the photo- and X-ray sensitivity of these solid solutions are higher than those of pure $TlGaS_2$. The nature of dielectric losses and the hopping mechanism of charge transport in the $(TlGaS_2)_{1-x}(TlInSe_2)_x$ solid solutions have been established from the experimental results on high-frequency dielectric measurements. The temperature dependences of exciton peak position for various compositions (x = 0…0.3) have been investigated within 77…180 K temperature interval. It has been ascertained that, with increasing x in $(TlGaS_2)_{1-x}(TlInSe_2)_x$ solid solutions, the width of their forbidden gap decreases.

Keywords: solid solutions, photosensitivity, dielectric losses, exciton peak, X-ray dosimetry.

Manuscript received 30.11.16; revised version received 16.01.17; accepted for publication 01.03.17; published online 05.04.17.

1. Introduction

Ternary layer-chain $TlGaS_2$ and $TlInSe_2$ single crystals exhibit high photo- and X-ray sensitivity making them well-suited for photoresistors and X-ray detectors [1-4]. The study of physical properties of the $TlGaS_2$, $TlInSe_2$ compounds and solid solutions on their base are very important for ascertaining the relations between their compositions and properties. This offers the possibility of controlling the band gap, energy position of emission bands and electrical conductivity of these semiconductors. In [5-7] the results of investigations of *ac* electric and dielectric properties of $TlGaS_2$, $TlInSe_2$ and diluted $(TlGaS_2)_{1-x}(TlInSe_2)_x$ solid solutions (x = 0.005 and 0.02) are given.

The purpose of this work was to investigate the influence of $(TlGaS_2)_{1-x}(TlInSe_2)_x$ solid solutions compositions (x = 0…0.5) on their photo- and X-ray sensitivity, *ac* electric, dielectric and optical properties.

2. Experimental

The synthesis of $(TlGaS_2)_{1-x}(TlInSe_2)_x$ solid solutions was carried out in ampoules evacuated to the pressure 10^{-3} Pa. The ampoule was fabricated from a fused silica tube. In this case, $(TlGaS_2)_{1-x}(TlInSe_2)_x$ samples were

Semiconductor Physics, Quantum Electronics & Optoelectronics, 2017. V. 20, N 1. P. 74-78.
doi: https://doi.org/10.15407/spqeo20.01.074

Table 1. Crystal data for $TlGaS_2$ and $(TlGaS_2)_{1-x}(TlInSe_2)_x$.

Solid solution composition	*a*(Å)	*b*(Å)	*c*(Å)	β	*Z*	Space group
$TlGaS_2$	10.40	10.40	15.17	100.06°	16	$P2_{1/n}$
$(TlGaS_2)_{0.9}(TlInSe_2)_{0.1}$	10.40	10.40	15.18	100.06°	16	$P2_{1/n}$
$(TlGaS_2)_{0.8}(TlInSe_2)_{0.2}$	10.41	10.41	15.18	100.06°	16	$P2_{1/n}$
$(TlGaS_2)_{0.7}(TlInSe_2)_{0.3}$	10.43	10.43	15.181	100.06°	16	$P2_{1/n}$
$(TlGaS_2)_{0.6}(TlInSe_2)_{0.4}$	10.435	10.435	15.20	100.06°	16	$P2_{1/n}$
$(TlGaS_2)_{0.5}(TlInSe_2)_{0.5}$	10.452	10.452	15.245	100.06°	16	$P2_{1/n}$

prepared due to interaction of initial components ($TlGaS_2$ and $TlInSe_2$). To prevent the ampoule filled with reactants from explosion, the furnace temperature was raised to the melting temperature of selenium (T = 493 K), and the ampoule was held at this temperature for 3 h. Then, the furnace temperature was raised up to T = 1080 K at the rate close to 50 K/h, and the ampoule was kept at this temperature for 4 h, after which it was cooled down to 300 K at the rate 20 K/h. Phase purity of $(TlGaS_2)_{1-x}(TlInSe_2)_x$ was determined using the differential thermal analysis and powder X-ray diffraction. Each sample was used as the charge for Bridgman crystal growth. The crystal data for $(TlGaS_2)_{1-x}(TlInSe_2)_x$ are presented in Table 1.

The spectral characteristics of photoresponse were recorded with a GIBI-TIBI potentiometer; the samples being illuminated with a 400-W incandescent lamp through the DMR-4 monochromator.

In X-ray dosimetry measurements, we used a URS-55 X-ray generator. Variation of the sample resistance under X-ray irradiation was followed with the R-4053 bridge. X-ray dose rates were measured with a DRGZ-02 dosimeter.

Measurements of the dielectric properties of $(TlGaS_2)_{1-x}(TlInSe_2)_x$ (x = 0.1, 0.2) single crystals were performed at fixed frequencies within the range $5\cdot10^4\ldots3.4\cdot10^7$ Hz by the resonant method using TESLA BM560 Q-meter. The monocrystalline samples for dielectric measurements had the form of planar capacitors normal to the *C*-axis of the crystals, with silver paste electrodes. The thickness of the crystal samples was 90 to 120 μm, and the area of the capacitor plates was $8\cdot10^{-2}\ldots2\cdot10^{-1}$ cm^2. All dielectric measurements were performed at the temperature T = 300 K. The accuracy in determining the resonance capacitance and the quality factor Q = 1/tanδ of the measuring circuit was limited by errors related to resolution of the device readings. The accuracy of the capacitor graduation was ±0.1 pF. The reproducibility of the resonance position was ±0.2 pF in capacitance and ±(1.0…1.5) scale divisions in quality factor. The largest deviations were 3-4% in ε and 7% in tanδ.

Optical absorption spectra were measured using the samples in the form of platelets 10–100 μm thick cleaved from the monocrystalline ingots. Light was incident along the normal to the layers of the samples, that is, along the crystallographic axis *C* of the crystals. Optical transmission spectra were measured as functions of temperature using the experimental setup built around a KSVU-6M system and UTREKS helium cryostat, which ensured temperature stabilization with the accuracy ±0.01 K. The setup included the MDR-6 double monochromator and FEU-100 photomultiplier tube. The spectral resolution of the experimental configuration was equal to 2 Å.

3. Results and discussion

We measured spectral dependences of photoconductivity and photosensitivity R_d/R_{ph} (R_d is the dark resistance, and R_{ph} is the resistance of the sample under above-gap illumination) at a steady illumination, as well as the X-ray sensitivity and other photoelectric parameters. Table 2 and Fig. 1 give the photoelectric properties of the $(TlGaS_2)_{1-x}(TlInSe_2)_x$ solid solutions.

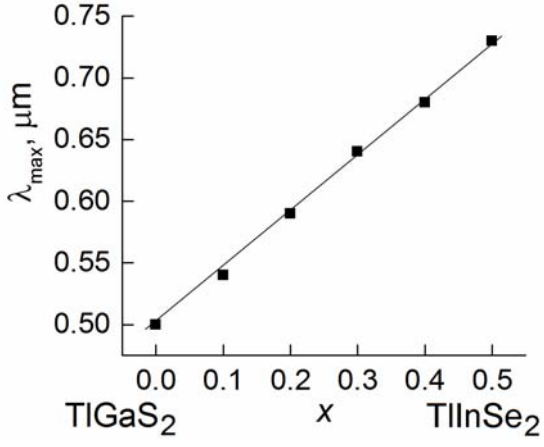

Fig. 1. Composition dependence of the photosensitivity maximum in $(TlGaS_2)_{1-x}(TlInSe_2)_x$ solid solutions.

Table 2. Photoelectric and X-ray dosimetric characteristics of the $(TlGaS_2)_{1-x}(TlInSe_2)_x$ solid solutions.

Solid solution composition	$\Delta\lambda_{max}$, μm	R_d, Ohm	R_d/R_{ph} at 200 lx	K_σ, min/R
$TlGaS_2$	0.46–0.57	$(3…5)\cdot10^{10}$	5–8	0.063–0.159
$(TlGaS_2)_{0.9}(TlInSe_2)_{0.1}$	0.50–0.62	$(1…2)\cdot10^{10}$	10–25	0.075–0.178
$(TlGaS_2)_{0.8}(TlInSe_2)_{0.2}$	0.55–0.66	$(3…4)\cdot10^{9}$	15–30	0.089–0.198
$(TlGaS_2)_{0.7}(TlInSe_2)_{0.3}$	0.59–0.71	$(2…3)\cdot10^{8}$	21–37	0.098–0.213
$(TlGaS_2)_{0.6}(TlInSe_2)_{0.4}$	0.64–0.76	$(1…2)\cdot10^{7}$	23–42	0.107–0.219
$(TlGaS_2)_{0.5}(TlInSe_2)_{0.5}$	0.69–0.81	$(3…5)\cdot10^{6}$	25–46	0.142–0.252

From Fig. 1, one can see that the photosensitivity maximum (λ_{max}) linearly shifts from 0.50 to 0.73 μm when x increases from 0 to 0.5. This shift is associated with a decrease in the band gap with increasing x. This increase leads to a redshift of the sensitivity range $\Delta\lambda$ and a considerable rise in R_d/R_{ph} ratio under 200-lx illumination. For example, R_d/R_{ph} of $(TlGaS_2)_{0.5}(TlInSe_2)_{0.5}$ is 5 to 6 times higher than that of pure $TlGaS_2$ (Table 2). The rise in R_d/R_{ph} with increasing x is apparently related with an increase in both the lifetime and mobility of the photogenerated carriers.

Roengenosensitivity K_σ of $(TlGaS_2)_{1-x}(TlInSe_2)_x$ was characterized by the relative change in conductivity per unit dose rate,

$$K_\sigma = \frac{\Delta\sigma_{E,0}}{\sigma_0 \cdot E}, \qquad (1)$$

where σ_0 is the conductivity of the unirradiated crystal and $\Delta\sigma_{E,0} = \sigma_E - \sigma_0$ is the change in the conductivity under X-ray irradiation with the dose rate E (R/min). Table 2 lists K_σ values corresponding to the accelerating voltages from 25 to 30 keV and dose rates from 0.75 to 10 R/min. One can see that K_σ of $(TlGaS_2)_{1-x}(TlInSe_2)_x$ solid solutions exceeds that of pure $TlGaS_2$. As the $TlInSe_2$ content increases, K_σ rises up to 0.142…0.252 min/R at $x = 0.5$.

We measured also the electric capacitance of $(TlGaS_2)_{0.9}(TlInSe_2)_{0.1}$ and $(TlGaS_2)_{0.8}(TlInSe_2)_{0.2}$ samples within the frequency range $5\cdot10^4…3.4\cdot10^7$ Hz. Using the measured capacitances of these samples, we calculated the permittivity ε at different frequencies. The ε values of $(TlGaS_2)_{1-x}(TlInSe_2)_x$ single crystals vary from 9.5 to 12.7 for $x = 0.1$ and from 9.8 to 11.6 for $x = 0.2$ over the entire frequency range studied, with no significant dispersion (ε of $TlGaS_2$ single crystal, as it was shown in [5], varies from 26 to 30 at $f = 5\cdot10^4…3\cdot10^7$ Hz).

In contrast to that reported for $TlGaS_2$ in [5], the frequency dependences of the loss tangent for the $(TlGaS_2)_{1-x}(TlInSe_2)_x$ ($x = 0.1$, 0.2) single crystals have maxima, which are indicative of relaxation losses [8].

The *ac* conductivity of investigated samples varies as $f^{0.8}$ at $f = 5\cdot10^4…2\cdot10^6$ Hz for $x = 0.1$ and at $f = 5\cdot10^4…6\cdot10^6$ Hz for $x = 0.2$. At higher frequencies, $\sigma_{ac}(f)$ – dependence of these crystals was superlinear ($\sim f^{1.4}$).

The $\sigma_{ac} \sim f^{0.8}$ dependence indicates that the mechanism of charge transport is hopping over localized states near the Fermi level [9].

$$\sigma_{ac}(f) = \frac{\pi^3}{96} \cdot e^2 kT N_F^2 a^5 f \left[\ln\frac{\nu_{ph}}{f}\right]^4, \qquad (2)$$

where e is the elementary charge, k – Boltzmann constant, N_F – density of localized states near the Fermi level, $a = 1/\alpha$ – localization length, α – decay parameter of the wave function of a localized charge carrier, $\psi \sim e^{-\alpha r}$, and ν_{ph} – phonon frequency.

Using the expression (2), we can calculate the density of states at the Fermi level from the measured values of the conductivity $\sigma_{ac}(f)$. The calculated values of N_F for $(TlGaS_2)_{1-x}(TlInSe_2)_x$ solid solutions ($x = 0.1$, 0.2) single crystals were given in Table 3 (localization radius is chosen as 14 Å, by analogy with the $TlGaS_2$ single crystal [5]).

According to the theory of hopping conduction, we calculated the mean hop distance (R) and mean hop time (τ) in an applied *ac* electric field using the formula [9]:

$$\tau^{-1} = \nu_{ph} \exp(-2R\alpha), \qquad (3)$$

where R is the average hopping distance,

$$R = \frac{1}{2\alpha}\ln\frac{\nu_{ph}}{f}. \qquad (4)$$

These values are also adduced in Table 3.

Knowing N_F and R from [9]:

$$\frac{4\pi}{3} R^3 N_F \cdot \frac{\Delta E}{2} = 1, \qquad (5)$$

we estimated scattering of energies inherent to trap states near the Fermi level (ΔE): $\Delta E = 0.075$ eV for $x = 0.1$ and 0.085 eV for $x = 0.2$. The evaluated concentrations of deep traps determining the *ac* conductivity of $(TlGaS_2)_{1-x}(TlInSe_2)_x$ single crystals ($N_t = N_F \cdot \Delta E$) are given in the last column of Table 3. It is seen from this table that, with increase of x from 0 to 0.2 in $(TlGaS_2)_{1-x}(TlInSe_2)_x$ single crystals, the values of N_F and N_t increase, while R decreases.

Optical properties of $(TlGaS_2)_{1-x}(TlInSe_2)_x$ ($x = 0…0.3$) single crystals were studied in 77 to 180 K temperature interval. The thicknesses of crystals under study were 20–50 μm. Light was incident on the crystals in direction parallel to their crystallographic axis *C*.

The obtained data on the optical properties of the $(TlGaS_2)_{1-x}(TlInSe_2)_x$ demonstrate that, at temperatures from 77 to 180 K, crystals have the absorption band near fundamental absorption edge, which is due to transitions into the direct exciton state. We examined the temperature dependence for the energy position of the exciton peak for $(TlGaS_2)_{1-x}(TlInSe_2)_x$ crystals within the temperature range 77…180 K (Fig. 2). It is seen that the peak position of the exciton band of $(TlGaS_2)_{1-x}(TlInSe_2)_x$ solid solutions has a positive temperature coefficient. Since the exciton energy is a weak function of temperature, it indicates that the band gap of $(TlGaS_2)_{1-x}(TlInSe_2)_x$ crystals increases with temperature.

Table 3. Parameters of $(TlGaS_2)_{1-x}(TlInSe_2)_x$ single crystals obtained from high-frequency dielectric measurements.

Crystal composition	N_F, $eV^{-1}\cdot cm^{-3}$	τ, s	R, Å	N_t, cm^{-3}
$TlGaS_2$	$2.1\cdot10^{18}$	$2\cdot10^{-6}$	103	$4.2\cdot10^{17}$
$(TlGaS_2)_{0.9}(TlInSe_2)_{0.1}$	$6.8\cdot10^{18}$	$9.8\cdot10^{-7}$	98	$5.1\cdot10^{17}$
$(TlGaS_2)_{0.8}(TlInSe_2)_{0.2}$	$7.7\cdot10^{18}$	$3.3\cdot10^{-7}$	90	$6.5\cdot10^{17}$

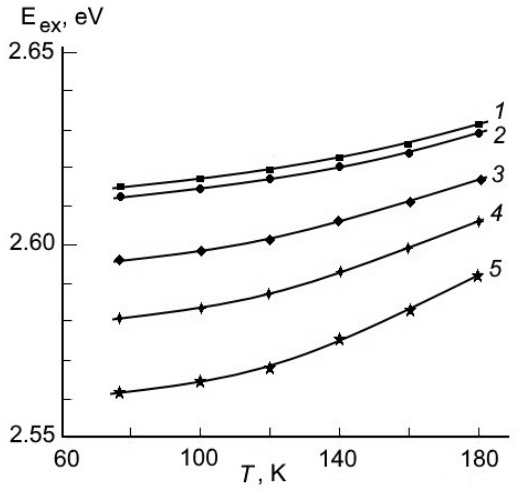

Fig. 2. Temperature dependences of the energy position of the exciton peak at the absorption edge of $(TlGaS_2)_{1-x}(TlInSe_2)_x$ solid solutions: $x = 0$ (*1*), 0.02 (2), 0.1 (*3*), 0.2 (*4*), 0.3 (*5*).

Temperature variation of the band gap in semiconductors E_g is known to be defined by a combined effect of thermal expansion of their lattice and electron-phonon interaction. Semiconductors rarely have a positive temperature coefficient of their band gap. In particular, such an experimental fact in $TlGaS_2$ and $TlGaS_2$-based single crystals [10, 11] is thought to be caused by significant contribution of thermal expansion of their lattice to the temperature variation of E_g. Thus, the $TlGaS_2$ and $(TlGaS_2)_{1-x}(TlInSe_2)_x$ crystals are found to be similar in the structure of their absorption edge formed by direct interband transitions.

4, Conclusions

The results of photoelectric, X-ray dosimetric and high-frequency dielectric measurements with prepared $(TlGaS_2)_{1-x}(TlInSe_2)_x$ solid solutions provided an opportunity to increase photo- and X-ray sensitivity, to determine the mechanism of dielectric losses and charge transport, as well as to evaluate the density of localized states at the Fermi level, the average time of charge carrier hopping between localized states, average hopping distance, scattering of trap states near the Fermi level and concentration of deep traps responsible for *ac* conductivity. The temperature dependences of exciton peak position for $(TlGaS_2)_{1-x}(TlInSe_2)_x$ solid solutions were investigated within the temperature interval 77…180 K. It has been ascertained that the edge of optical absorption in these solid solutions is formed by vertical exciton transitions with the positive temperature coefficient.

References

1. Mustafaeva S.N., Kerimova E.M., Ismailova P.G., Asadov M.M. Roentgendosimetric characteristics of detectors on the base of $TlGaS_2\langle Yb\rangle$ single crystals. *Fizika*. 2004. **10**, No. 4. P. 108–115.
2. Kerimova E.M., Mustafaeva S.N., Asadov Yu.G., Kerimov R.N. Synthesis, growth and properties of $TlGa_{1-x}Yb_xS_2$ crystals. *Crystallography Reports*. 2005. **50**, No. 1. P. 122–123.
3. Mustafaeva S.N. Photoelectric and X-ray dosimetric properties of $TlGaS_2\langle Yb\rangle$ single crystals. *Physics of the Solid State*. 2005. **47**, No. 11. P. 2015–2019.
4. Mustafaeva S.N., Kerimova E.M., Asadov M.M., Kerimov R.N. Roentgenodetectors on the base of $TlInSe_2\langle Li^+\rangle$. *Fizika*. 2003. **9**, No. 3, 4. P. 62–64.
5. Mustafaeva S.N. Frequency dispersion of dielectric coefficients of layered $TlGaS_2$ single crystals. *Physics of the Solid State*. 2004. **46**, No. 6. P. 1008–1010.
6. Mustafaeva S.N. Frequency dependence of real and imaginary parts of complex dielectric permittivity and conductivity of $TlInSe_2$ single crystal at relaxation processes. *J. Radioelectron.* 2013. **7**. P. 1–8.

7. Mustafaeva S.N. Frequency effect on the electrical and dielectric properties of $(TlGaS_2)_{1-x}(TlInSe_2)_x$ (x = 0.005, 0.02) single crystals. *Inorganic Materials*. 2010. **46**, No. 2. P. 108–111.
8. Pasynkov V.V. and Sorokin V.S. *Materials of Electronic Engineering*. Lan' Publishing, 2004. 368 p. (in Russian).
9. Mott N. and Davis E. *Electron Processes in Noncrystalline Materials*. Clarendon Press, Oxford, 1971. 472 p.
10. Mustafaeva S.N., Asadov M.M., Kyazimov S.B., Gasanov N.Z. *T-x* phase diagram of the $TlGaS_2$–$TlFeS_2$ system and band gap of $TlGa_{1-x}Fe_xS_2$ ($0 \le x \le 0.01$) single crystals. *Inorganic Materials.* 2012. **48**, No. 10. P. 984–986.
11. Mustafaeva S.N., Asadov M.M., Kerimova E.M., Gasanov N.Z. Dielectric and optical properties of $TlGa_{1-x}Er_xS_2$ (x = 0, 0.001, 0.005, 0.01) single crystals. *Inorganic Materials*. 2013. **49**, No. 12. P. 1175–1179.